NHTC2000-12219

INVESTIGATION OF THE REYNOLDS STRESS AND VELOCITY FIELD IN A RIB ROUGHENED CHANNEL USING LASER DOPPLER VELOCIMETRY

MAURIZIO VALLA
POLITECNICO OF MILAN

EDWARD HUCKLE
MAE DEPT. UCLA

KUNZHONG HU
MAE DEPT. UCLA

STANLEY JONES
MAE DEPT. UCLA

VLADIMIR TRAVKIN
MAE DEPT. UCLA

IVAN CATTON
MAE DEPT. UCLA

KEYWORDS: *LDV, TURBULENCE, REYNOLDS STRESS, CHANNEL WALL ROUGHNESS*

ABSTRACT

Laser Doppler Velocimetry (LDV) was used to measure the turbulent velocity field in a rib-roughened internal channel flow. Measurements were taken in a section between two consecutive ribs and from the centerline to the top of the test section. The test section was comprised of a rectangular duct with ribs of square cross section mounted (transverse flow) on the top and bottom channel surfaces. Five distributions of ten points each (more concentrated in the rough sub-layer) were measured. Data were collected for two components of velocity, allowing calculation of the Reynolds stress. Additionally, photos of the particle deposition patterns were taken and compared to the quantitative results.

NOMENCLATURE

a	= 50 mm, duct height
b	= 150 mm, duct width
d_{PV}	probe volume width
l_{PV}	probe volume length
f	frequency
h	half height of the channel
H	rib height
M	vector/array magnitude
P	rib pitch
Re	Reynolds number
S/N	signal to noise ratio
t	time
u, (U)	instantaneous (mean) velocity in x-direction
u'	velocity fluctuation in the x-direction
v, (V)	instantaneous (mean) velocity in y-direction
v'	velocity fluctuation in the y-direction
y^*	= y / (a/2)
p	wet perimeter
u_b	bulk velocity
u_τ	friction velocity
K_S	equivalent roughness
f^*	friction factor

Greek Symbols

δ	fringe spacing
μ	dynamic viscosity
ρ	density
τ_S	shear stress

INTRODUCTION

The study of turbulent flow and its characteristics has been the subject of a large number of investigations in many fields of the research and applications. In the past 20 years several researchers contributed to the experimental study of flow and heat transfer in rib roughened ducts. Among others there are Olsson and Sunden (1998), Hwang and Liou (1994 and 1995), Liou et al. (1990), Liou et al. (1995), Zhang et al. (1995), Han (1988) and Rosen and Tragardh (1994). Different experimental techniques were applied in their studies and a large selection of geometries were investigated. Holographic Interferometry, Particle Image Velocimetry (PIV), and Laser Doppler Velocimetry are widely used in these investigations. The rough channel with rectangular ribs and other rib profiles is a common subject of experimental

works, but few of those present investigations of the Reynolds stress.

Experimentally obtaining the Reynolds stress requires measurement of the two velocity components of the flow in the same position at the same time. In this study this was achieved by the use of an experimental technique called Laser Doppler Velocimetry. Its unique feature is a non-intrusive probe that facilitates accurate, instantaneous velocity measurements, which is of particular importance for turbulent measurements.

From a theoretical point of view theories and models were developed to solve the turbulent flow problem. The Navier-Stokes system of equations for turbulent flow presents a number of unknowns greater than the number of equations. Closure to this problem may be accomplished by empirical evaluation of the Reynolds stress.

The purpose of this study was the experimental investigation of the Reynolds stress in the rough channel with the LDV measuring technique. The Reynolds stress investigation implies the obtainment of the mean velocity (both components) and its fluctuating part.

This paper has several parts. First, the optical technique of Laser Doppler Velocimetry (LDV) followed by the experimental wind tunnel apparatus are described. The signal analysis is briefly discussed and the location of the measurement nodes is specified. The results section consists of plots of the mean and fluctuating u and v velocity components as well as the Reynold stress. Finally, an interesting picture of particle deposition is shown, and conclusions are drawn.

EXPERIMENTAL APPARATUS

LDV System

A Spectra Physics model 165 argon-ion laser, operating in the multi-wavelength mode, was used to measure the instantaneous u- and v-velocity components of the flow (x- and y-direction, respectively).

After collimating the laser beams, color separation was accomplished by an equilateral prism. The green (514.5nm) and the blue (488nm) beams were selected and the other beams were truncated. The beams were then individually split (maintaining polarization) using cube beam-splitters. The green beams were passed through Bragg cells allowing frequency shifting for directional sensitivity. Isomet model 1201-E acousto-optic modulators with 221A-2 drivers were used to amplitude modulate the beams at 43MHz and 40MHz, respectively. This 3MHz difference causes the fringes in the probe volume to move in a known direction, allowing distinction between positive and negative v-velocities. Green light (λ=514.5 nm) was chosen for the v-component (y-direction) of velocity. This is due to the fact that, since green beam has the strongest intensity it is better suited for frequency shifting. This operation causes an intensity attenuation and also a reduction in size (the Acousto Optic Modulator aperture is of 1.56 mm only).

To make measurements as close to the top wall as possible the standard 2 component configuration (with all 4 beams symmetrical in a cross) was altered. The upper green beam was moved to the center, therefore the 4 beams were in a T-formation as they passed through the transmitter lens, as seen in Figure 1.

This configuration of the green beams (for measuring the v-component) causes an angular deviation from the orthogonality of the fringe plane. As stated in reference [1], the difference between the measured velocity and the velocity in the normal direction can be considered negligible.
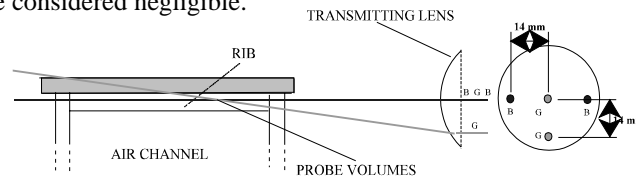
Figure 1: Crossing beam configuration

This configuration of the green beams, spaced 14 mm apart, were focused into the probe volume using a 300 mm focal length transmitter lens. This led to a fringe spacing (δ_{green}) of 11 microns with 8 fringes total, and a probe volume width (d_{PV}) of 85 microns and a length (l_{PV}) of 3.66 mm. Similarly, for the blue beams, a beam spacing of 28 mm gave a fringe spacing (δ_{blue}) of 5.2 microns with 14 fringes total, a probe volume width of 74 microns and a length of 1.6mm. The alignment of the four crossing beams was confirmed using a small wire mounted on a rotating wheel.

A backscatter receiver configuration utilizing the transmitter lens to collect and collimate the scattered light was used. A dichroic mirror separated the green from the blue color. These colors were then focused into two fiber-optic cables and into photo-multiplier tubes. The alignment was then controlled utilizing the rotating wheel with the LabView program. Figure 2 shows the 2-color (component) LDV system.
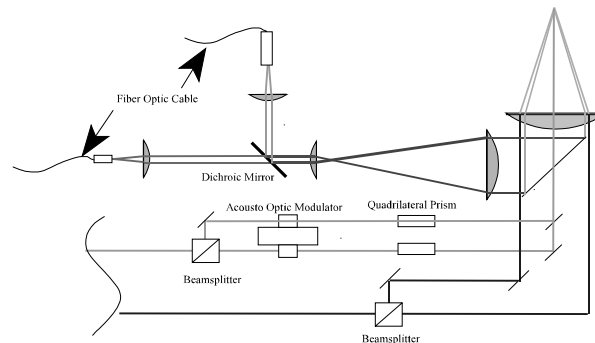
Figure 2 LDV system

THE WIND TUNNEL

The wind tunnel apparatus was an open loop that propelled air flow through the test section. The tunnel consists of a centrifugal blower with a speed controller, a particle feeder, a test section and a particle recoverer that utilized a HEPA filter. The test section consisted of three principal ducts: an entrance duct for the development of the flow, the test section duct and a duct to ensure that a sudden change of the cross-section does not effect the flow. For the test section construction, 0.25 inch thick plexiglass was used. It was 1500 mm long with a cross section of 150 mm

(depth) x 50 mm (height). Twenty ribs (6.35 mm x 6.35 mm) were regularly arranged (spaced every 75 mm) on opposite sides (top and bottom) of the duct. The entrance duct had a length of 1500 mm long with a rectangular cross section 150 mm (depth) x 50 mm (height). The length of the entrance duct, in order to stabilize the flow, corresponded to 20 hydraulic diameters. Figure 3 shows the entire wind tunnel.
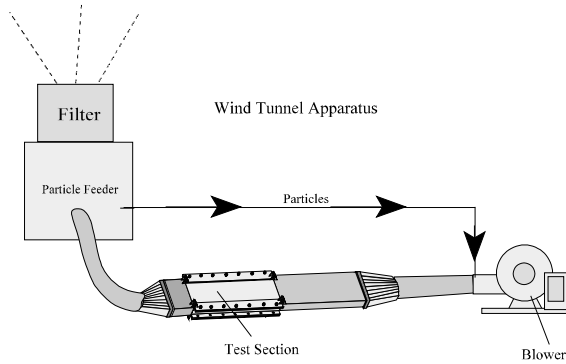
Figure 3: Wind tunnel

SIGNAL PROCESSING

The electronic signals were first amplified with two Stanford Systems model SR445 pre-amplifiers and then digitized using a Gage Compuscope 265 A/D card. The LabView 4.1 Full Development Studio was used both for A/D card hardware control and also for the signal processing needs.

The raw digitized signals were displayed for visual user verification of burst quality. The signals were next filtered using Butterworth bandpass filters for the low frequencies (pedestal: always present in LDV signals) and the high frequencies removal (Noise). Digital power spectrums were then performed on the filtered signals in order to determine the burst frequencies, proportional to the velocity components. In order to mathematically quantify the quality of each burst a signal to noise criteria was developed, and is given by:

$$S/N = \frac{M_{signal}}{M_{noise}} \qquad (1)$$

For this relation, M correspond to the magnitude of a vector array (evaluated using an inner product). The power spectrum of an LDV signal is a delta function at the burst frequency. Thus, M_{signal} was the magnitude of the sub-array surrounding the delta function, and M_{noise} is the magnitude of the remaining power spectrum array. Signals of excellent quality (greatly resembling a delta function) would have a very high S/N (at least 10 or 100) whereas poor signals would have a S/N of less than unity. This enabled post - filtering based on a minimum S/N criteria. The data was also manually post - filtered to exclude the small occurrences of signals with high S/N but unrealistic frequencies (caused by multiple particles in the probe volume or other spurious signals). For each data point a statistically significant number (100 - 500) of samples were taken (each consisting of a burst frequency realization and burst S/N) and statistical information was calculated.

EXPERIMENTAL RESULTS

This section presents the results obtained and the necessary post processing in order to validate and show the consistency of the entire project. Since few correlations or experimental works have been developed for similar investigations, comparison of the results with the current literature is not easily realized. For this reason the main objective of this section is to validate, as much as possible, the results, try to justify the experimental assumptions, and underline the points of uncertainty.

Measurements

Measurements were taken in the section between two ribs and from the centerline to the top wall of the test section. A number of assumptions were made. First, the flow was assumed to be perfectly symmetric with respect to the centerline. This allowed for measurement of only the upper part of the test section and thus avoiding the excessive particle deposition. Secondly it is assumed that a repetitive flow pattern between successive sets of ribs (the flow is considered fully developed). Additionally the flow is assumed to be 2-dimensional which implies that the lateral walls of channel do not influence the flow.
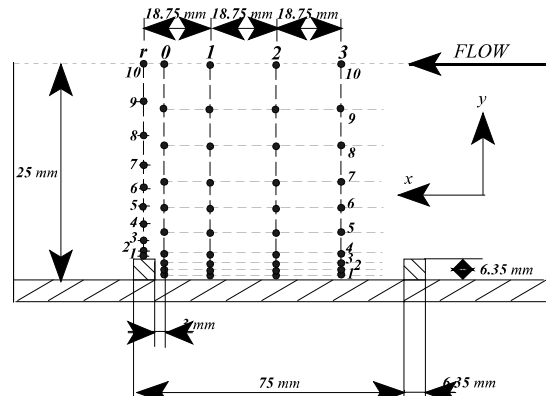
Figure 4 Measuring points

As shown in Figure 4 (the grid is represented in the lower part of the test section for simplicity), five distributions were taken from the centerline to the top (named r,0,1,2,3 - see Figure 4), with ten points for each distribution. These points are numbered from 1 to 10, respectively, from the top to the centerline. For these series of measurements the speed controller of the blower was set to 30 Hz in order to achieve a Reynolds number around 25,000.

Results

The results were all nondimensionalized: for the U and V-component the maximum $\bar{U}$-value of "r distribution" was used (U_{ref}=6.025 m/s).
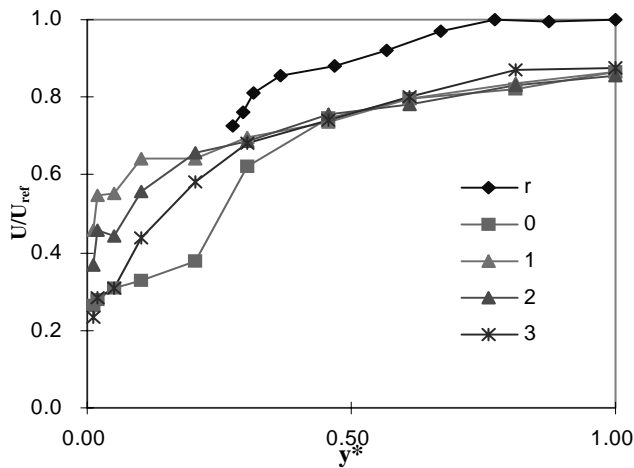
Figure 5: Nondimensional U-components profiles

Figure 5 shows the distributions obtained for the U-component of velocity. As can be seen the distributions are typical of the turbulent flow with a flat trend near the centerline of the tunnel and a large gradient close to the wall. This is a sign of the acceleration of the flow due to the changing cross sectional area for the presence of the rib (see picture of the particle deposition). For this purpose, this figure illustrates the conservation of mass along the channel. In the immediate neighborhood of the wall (or the bottom of the rib) the crossing beam disposition allowed a good access of the LDV optics. Therefore, several measurements were taken in the boundary layer. In the figure the Reynolds number is defined as

$$Re \cong \frac{4 \rho \, u_b \, h(x)}{\mu} \quad , \qquad (2)$$

where u_b is the bulk velocity evaluated as follows:

$$u_b = \frac{1}{h} \int_0^h u(y) \, dy \quad , \qquad (3)$$

Figure 6 shows the distributions for the V velocity component.
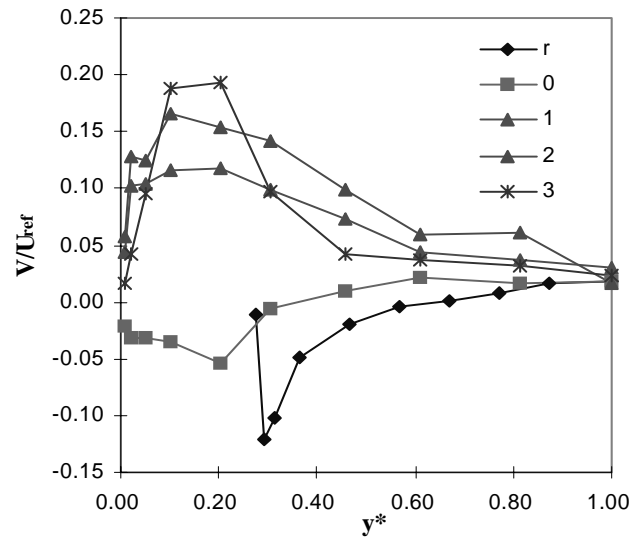
Figure 6: Nondimensional V-component profiles

The V-component presents velocity directional sensitivity and shows exactly the direction of the flow. As we expected in distributions r and 0 it is negative respectively near the rib and wall: this is due to the presence of the rib that suddenly changes the direction of the fluid element, generating a vortex right after the rib itself.

Figure 7 shows the distributions obtained for the Reynolds stress.
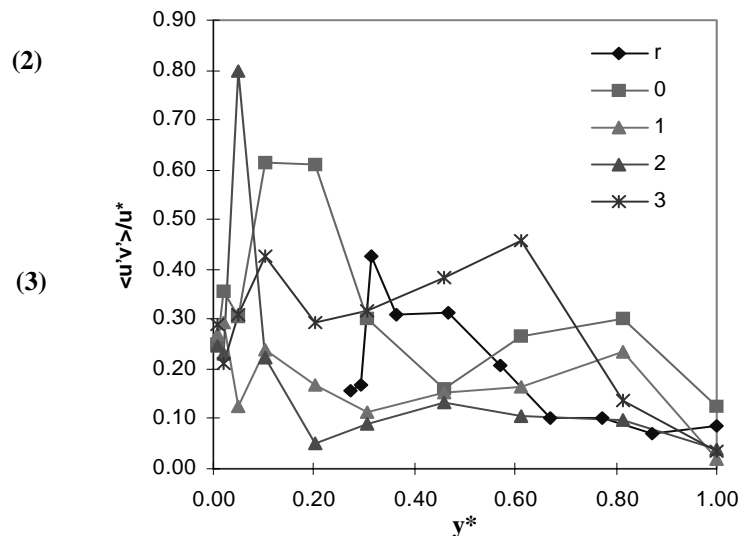
Figure 7: Nondimensional Reynolds stress profiles

The analysis of the Reynolds stress distribution is much more complicated by the lack of similar experimental works, limiting the possibility of comparisons. However, correlations and theories for the plain channel show a trend of the Reynolds stress that coincide with the present experimental data. In the measuring section a fluid element has both u' and v' fluctuating velocity components. On the

average, most of the particles with a positive value of u' have also a positive value of v' and vice versa; therefore the Reynolds stress is positive (see Figure 8). In the case of distribution r a force in the y-direction is exerted upon the fluid on the right side of the rib. This generates a vortex right after the rib in the flow direction.

In the viscous sublayer and in the buffer layer (close to walls and ribs) there is a very small perturbation of the velocity. Therefore, in the near wall region the Reynolds stress is supposed to be very small, meanwhile the shear stress is dominant. This is confirmed by the experimental data.

In the turbulent layer, the Reynolds stress is the dominating stress and it plays an important role on the fluid flow. It is due to the turbulent motion of the fluid flow itself. In the
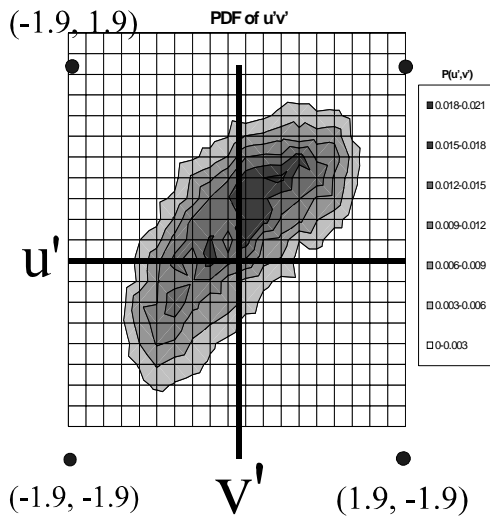
Figure 8: PDF of the Reynolds Stress for a generic measuring point

turbulent layer from the wall to the centerline the Reynolds stress shows a decreasing trend. This is caused by the turbulence that, approaching the centerline, becomes homogeneous: this means that there is no preferential direction in the movement of the fluid element. The plot of u' versus v' should show a scattered configuration concentrated in the origin of the axes and with samples equally distributed in the four quadrants. Figure 8 shows the probability density function and the scattered plot of a generic measuring point of this section. The range of this plot is -1.9 to 1.9 on both axes. Upon closer investigation of the data additional information about the Reynolds stress in the turbulent layer can be gleaned. An unaccountable feature of the data is that the U-velocity distribution close to the middle of the channel should be almost flat yet is found to be otherwise. This may be the cause for the discrepancy in the Reynolds stress results that should show a zero value at the centerline.

One of the biggest problems, but also an interesting feature of this experiment was the pattern of particle deposition. Although the deposited particles often decreased the visibility into the test section, at no time was the thickness of the deposited particles great enough to affect the flow. Through inspection of the film of particles stacked to the walls of the test section, a further confirmation of the results and of the assumptions was derived. The particles attached to the walls to form a repetitive

pattern that is characteristic of the flow in the rough channel. This pattern always had the same configuration in each cell (region between two successive rib sets). Figure 9 shows the repetition of the pattern. As can be seen in the figure, the pattern is repetitive along the channel; this is the best proof of the assumption of measuring only between two successive rib sets. From the figure it is easy to notice the different zones: the recirculating zone, created by the presence of the rib, the point of re-attachment and the zone of redevelopment of the flow.
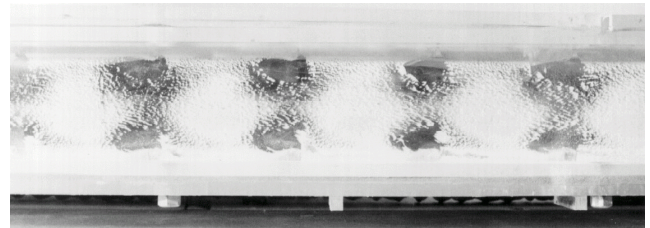
Figure 9: Repetitive pattern

In order to compare the results to the particle deposition a section (where the measurements were made) was enlarged from figure 9. This is shown in figure 10. When this picture was superposed onto the vector plot of velocity the two matched quite well. Looking at this picture it can be noticed the particle concentration gradient along the vertical axis. Besides that, the pattern presents a symmetric distribution that proves the assumption of measuring only in the upper part of the test section.
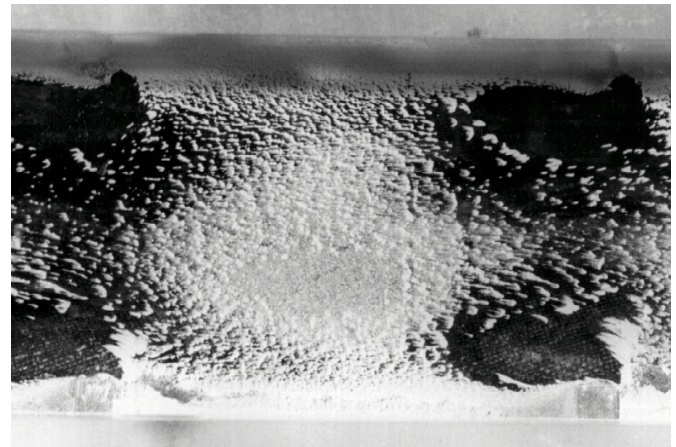
Figure 10: Closeup of area of measurement, showing particle deposition and symmetry.

CONCLUSION AND RECOMMENDATIONS

Considering the efforts made for an accurate and precise collection of data, the results obtained in the present experiment are more than satisfactory. They show the LDV measuring technique to be perfect for its features of non-intrusion and precision for fluid-dynamic investigations. Furthermore, the use of a skewed transmitter beam allowed measurements very close to the surfaces of walls and ribs. This method produced high quality burst signals exemplified by the high signal to noise ratios in the power spectrum analysis. On the other hand, this technique requires a perfect alignment and frequent control to maintain an elevated efficiency of the whole system. With this system measurements of two

components of velocity in the same time were performed. The data obtained were validated by the statistical analysis and the particle deposition. This analysis shows that enough samples in each measuring position were collected for the investigation of the mean velocities and their fluctuating parts. The Reynolds stress distributions reflect the expected trend, even if the lack of similar experimental works made the data analysis and its validation much more difficult. Furthermore, the velocity distributions show the typical direction of the flow in a rough channel with its characteristic zones: recirculating behind and after the rib, re-attachment and redevelopment zones. This division was visible in the pictures of the particle deposition that, besides several problems in the data acquisition phase, greatly helped in the post processing phase of the project.

Future experiments will investigate the recirculating zone with accurate flow resolution, different Reynolds numbers and flows between ribs of different height. Accurate flow resolution in the recirculating zone requires directional sensitivity for both components of velocity. In the experimental apparatus the u-directional detection was unavailable. In addition, different seeding particles will be used, which will alleviate the problem of particle deposition. Fiber optics for the transmitter of the LDV system would greatly speed up the data acquisition process, allowing micro-translation of the probe volume. Finally, the photo-multiplier tubes will be replaced by high sensitivity avalanche photodetectors for greater signal quality.

REFERENCES

Han, J. C., 1988, Heat Transfer and Friction Characteristics in Rectangular Channels with Rib Turbulators, *ASME Journal of Heat Transfer, Vol. 110, 321-328.*

Hwang, J. and Liou, T., 1994, Augmented Heat Transfer in a Rectangular Channel With Permeable Ribs Mounted on the Wall, *Journal of Heat Transfer, Vol. 116, 912-920.*

Hwang, J. and Liou, T., 1995, Heat Transfer and Friction in a Low-Aspect-Ratio Rectangular Channel With Staggered Perforated Ribs on Two Opposite Walls, *Journal of Heat Transfer, Vol. 117, 843-850.*

Liou, T., Chang, Y. and Hwang, D., 1990, Experimental and Computational Study of Turbulent Flows in a Channel With Two Pairs of Turbulence Promoters in Tandem, *Journal of Fluid Engineering, Vol. 112, 302-310.*

Liou, T., Wang, W. and Chang, Y., 1995, Holographic Interferometry Study of Spatially Periodic Heat Transfer in a Channel With Ribs Detached From One Wall, *Journal of Heat Transfer, Vol. 117, 32-39.*

Olsson, C. and Sunden, B., 1998, Experimental Study of Flow and Heat Transfer in Rib-Roughened Rectangular Channels, *Experimental Thermal and Fluid Science, Vol. 16, 349-365.*

Rosen, C. and Tragardh, C., 1994, $\langle u^{'} v^{'} \rangle$ Reynolds Stress in the Viscous Sublayer over a Wide Range of Re Numbers, *AIChE Journal, Vol. 40, No.1, 29-39.*

Zhang, Y. M., Gu, W. Z. and Han, J. C., 1994, Heat Transfer and Friction in Rectangular Channels With Ribbed or Ribbed-Grooved Walls, *Journal of Heat Transfer, Vol. 116, 58-65.*